J|A|C|S

A R T I C L E S

NMR Spectra of a Microcrystalline Protein at 30 kHz MAS

Matthias Ernst,[†] Andreas Detken,[†] Anja Böckmann,[‡] and Beat H. Meier*,[†]

Contribution from Physical Chemistry, ETH Zurich, CH-8093 Zürich, Switzerland, and Institut de Biologie et Chimie des Protéines, 7 passage du Vercors, F-69367 Lyon, France

Received July 1, 2003; E-mail: beme@ethz.ch

Abstract: Proteins are not always available in amounts desirable for solid-state magic-angle spinning (MAS) nuclear-magnetic resonance (NMR) spectroscopy. To maximize the signal-to-noise ratio achievable with small samples, the filling factor must be optimized by using small-diameter MAS rotors. These rotors have the added benefit of allowing higher radio frequency field amplitudes during polarization transfer steps and during decoupling periods as well as allowing higher spinning frequencies. We demonstrate the advantages of relatively fast MAS (30 kHz using a 2.5 mm rotor) compared to MAS at 12 kHz for the 10.4 kDa model protein Crh with 93 residues and show that the signal-to-noise ratio in two-dimensional correlation spectra can be significantly improved by taking advantage of optimized pulse sequences available with rapid MAS.

Introduction

Structure determination of proteins in microcrystalline or noncrystalline samples is an important challenge for solid-state NMR spectroscopy, and appropriate methods are currently being developed. Recently, the (almost) complete resonance assignment of solid-state magic-angle spinning (MAS) NMR spectra of small polypeptides with uniform or site-directed labeling[1-13] and a first solid-state NMR structure of a protein sample with site-directed labeling[14] have been published. The prerequisite for this development was the increased spectral resolution in multidimensional chemical-shift correlation spectra obtained by improved sample preparation techniques and recently developed spectroscopic methods.

For small amounts of protein, one of the major concerns is the low sensitivity of NMR leading to a low signal-to-noise (S/N) ratio in the spectrum. Currently, MAS rotors with an outer diameter (o.d.) of 4 mm and a sample volume of about 50 μL are the most common choices for solid-state NMR spectroscopy of peptides and proteins. For a 1D spectrum of a full rotor, we expect that the S/N ratio of a 2.5-mm rotor with a sample volume of about 11 μL is almost a factor of 3 lower than the S/N ratio of a 4-mm rotor. Here we have assumed that the S/N ratio per unit volume of a solenoid coil is proportional to the inverse of the coil diameter.[15,16] Experimentally, the decrease in the S/N ratio is found to be about a factor of 2. It should be pointed out, however, that the S/N ratio of the 1D spectrum is much less important than the S/N ratio of the cross-peaks in a 2D correlation spectrum since the information about connectivity and internuclear distances is contained in the cross-peaks. The cross-peak intensity in a 2D spectrum depends not only on the overall S/N ratio of the probe but also on the polarization transfer efficiency of the experiment.

Besides the sample volume, other important experimental conditions depend on the choice of the MAS rotor diameter. The maximum MAS frequency and the maximum radio frequency (rf) field amplitudes increase with decreasing rotor diameter. Going from a 4-mm to a 2.5-mm o.d. rotor increases the maximum spinning frequency from about 18 to 30 kHz, and the maximum rf field amplitude on the proton channel increases from about 100 to 150 kHz. For even smaller sample amounts, smaller and faster rotors are available[17] currently up to a maximum MAS frequency of 70 kHz.[18]

The higher MAS spinning frequencies and the higher radio frequency fields which can be used with smaller rotors contribute to an increased signal intensity of the cross-peaks in several ways. (i) Line intensity: the reduction in the number and in the intensity of spinning sidebands increases the center-band intensity. (ii) Line width: the separation of the spinning frequency from the closest $^{13}C-^{13}C$ rotational resonance condi-

[†] ETH Zurich.
[‡] Institut de Biologie et Chimie des Protéines.
(1) Straus, S. K.; Bremi, T.; Ernst, R. R. *J. Biomol. NMR* **1997**, *10*, 119−128.
(2) Detken, A.; Hardy, E. H.; Ernst, M.; Kainosho, M.; Kawakami, T.; Aimoto, S.; Meier, B. H. *J. Biomol. NMR* **2001**, *20*, 203−221.
(3) Straus, S. K.; Bremi, T.; Ernst, R. R. *J. Biomol. NMR* **1998**, *12*, 39−50.
(4) Hong, M. *J. Magn. Reson.* **1999**, *139*, 389−401.
(5) Hong, M. *J. Magn. Reson.* **1999**, *136*, 86−91.
(6) Hong, M. *J. Biomol. NMR* **1999**, *15*, 1−14.
(7) Hong, M. *J. Am. Chem. Soc.* **2000**, *122*, 3762−3770.
(8) McDermott, A.; Polenova, T.; Böckmann, A.; Zilm, K. W.; Paulsen, E. K.; Martin, R. W.; Montelione, G. T. *J. Biomol. NMR* **2000**, *16*, 209−219.
(9) Pauli, J.; van Rossum, B.; Forster, H.; de Groot, H. J.; Oschkinat, H. *J. Magn. Reson.* **2000**, *143*, 411−416.
(10) Pauli, J.; Baldus, M.; van Rossum, B.; de Groot, H.; Oschkinat, H. *ChemBioChem.* **2001**, *2*, 272−281.
(11) van Rossum, B.; Castellani, F.; Rehbein, K.; Pauli, J.; Oschkinat, H. *ChemBioChem.* **2001**, *2*, 906−914.
(12) Egorova-Zachernyuk, T. A.; Hollander, J.; Fraser, N.; Gast, P.; Hoff, A. J.; Cogdell, R.; de Groot, H. J. M.; Baldus, M. *J. Biomol. NMR* **2001**, *19*, 243−253.
(13) Böckmann, A.; Lange, A.; Galinier, A.; Luca, S.; Giraud, N.; Juy, M.; Heise, H.; Monserret, R.; Penin, F.; Baldus, M. *J. Biomol. NMR* **2003**, *27*, 323−339.
(14) Castellani, F.; van Rossum, B.; Diehl, A.; Schubert, M.; Rehbein, K.; Oschkinat, H. *Nature* **2002**, *420*, 98−102.
(15) Hoult, D. I.; Richards, R. E. *J. Magn. Reson.* **1976**, *24*, 71−85.
(16) Peck, T. L.; Magin, R. L.; Lauterbur, P. C. *J. Magn. Reson., Ser. B* **1995**, *108*, 114−124.
(17) Samoson, A.; Tuherm, T.; Past, J. *J. Magn. Reson.* **2001**, *149*, 264−267.
(18) Samoson, A.; Turhem, T. Presented at the 44th Experimental NMR Conference, Savannah, GA, 2003; Poster PJ 421.

tion in the spectrum is increased, eliminating unwanted line broadening from ^{13}C homonuclear couplings in uniformly labeled samples. The efficiency of heteronuclear decoupling of the ^{13}C or ^{15}N spins from the protons depends on the MAS frequency, the rf field strength, and the decoupling method employed[19-23] and, typically, also increases with increasing MAS frequencies. Multiple-pulse decoupling methods such as TPPM[21] or XiX[22,24] allow one to obtain efficient decoupling at high MAS frequencies with much lower decoupling fields than would be necessary using cw decoupling. (iii) Polarization transfer efficiency: many adiabatic polarization transfer schemes,[25] which in theory allow transfer efficiencies up to 100%, work best at high spinning frequencies. For example, the bandwidth of homonuclear recoupling using the DREAM method[26,27] increases with increasing MAS frequency.

Higher radio frequency fields become more accessible in small-diameter MAS probes due to the correspondingly smaller coil diameter. However, rf irradiation induces sample heating through the electrical part of the rf field especially if the sample has a high salt content. Heating through rf irradiation has to be minimized by implementing polarization transfer and decoupling schemes with reduced rf power requirements. Such schemes have recently been introduced for polarization transfer[26,27] and decoupling[19,28] under fast MAS, and their efficiency increases with increasing MAS frequency. We will employ the former, while the latter requires even faster MAS frequencies to be competitive in a sample with inherently narrow lines. At high spinning frequencies, present rotor/stator MAS assemblies suffer from significant heating.[29,30] At the maximum rotor speed for a given rotor diameter, heating by 20−30 K is observed and must be compensated by cooling.

A key factor for the line width observed in the spectrum is the sample preparation which determines the structural homogeneity of the sample.[2,10,13] Concerns have been raised that the forces encountered in fast MAS may compromise the sample quality, but we have encountered no such problems in the course of our study.

The model compound investigated here is the 10.4 kDa catabolite repression histidine-containing phosphocarrier protein (Crh) from *Bacillus subtilis*. The structure of Crh has been solved both by liquid-state NMR (monomeric form[31]) and by X-ray crystallography (domain swapped dimeric form[13]).

Sequential solid-state NMR assignments of the dimer have been obtained recently[13] using spectra obtained at 500 and 600 MHz, with 11 kHz MAS in a 4-mm o.d. rotor.

In this paper, we present homonuclear correlation spectra using a sample of 4 mg protein at an MAS frequency of 30 kHz and a decoupling field of 150 kHz. We assess the gain in S/N caused by fast MAS by comparing the S/N of the correlation cross-peaks in homonuclear chemical-shift correlation spectra using proton-driven spin diffusion at low MAS frequencies and adiabatic polarization transfer schemes using the DREAM method at high MAS frequencies. We found significant improvements in the S/N ratio at high MAS frequencies.

Experimental Section

The sample preparation of the Crh protein for solid-state NMR measurements was done as described in ref 13. In brief, Crh was overexpressed with a C-terminal LQ(6×His) extension.[32] Uniformly [^{13}C,^{15}N] labeled protein was obtained by growing bacteria in Silantes growth media. The protein was purified,[33] and Crh-containing fractions were dialyzed against 20 mM NH_4HCO_3. Microcrystalline Crh was prepared by slow precipitation of the protein with a 20% solution of PEG 6000, 0.02% NaN_3 in 20 mM NH_4HCO_3 over a 2 M NaCl reservoir solution. Resulting microcrystals were directly centrifuged into a 2.5-mm Bruker rotor, and rotor caps were sealed with super glue. The rotor used in this study contained about 4 mg of protein. The above conditions were optimized to ensure a low salt content of the sample to minimize sample heating by rf irradiation.

Spectra were collected on a Bruker 600 MHz wide-bore spectrometer using a commercial 2.5-mm triple-resonance probe by the same manufacturer. The sample was cooled by a separate cooling nitrogen stream with a flow of about 2000 L/h. The effective sample temperature was deduced from calibration measurements with a $Sm_2Sn_2O_7$ sample[29,30,34] as a function of spinning frequency and the set temperature of the nitrogen cooling stream. To obtain a sample temperature of 5 °C, the temperature of the nitrogen stream had to be set to −10 °C and −45 °C for the MAS frequencies of 12 and 30 kHz, respectively. The estimated temperature gradient over the sample and the accuracy of the temperature setting were both about 5 °C.

For the 1D spectra, 1024 scans were added up. The spectral width was set to 100 kHz, and 3072 complex data points were acquired. The cross-polarization time was 1 ms. The rf field amplitude for all hard pulses was set to 100 kHz (5 μs 180° pulse). The recycle delay was 3 s, leading to an acquisition time of about 1 h. The spectra were Fourier-transformed with zero filling to 64 k data points without applying a window function and were phase and baseline corrected.

For the 2D spectra, 80 scans were added up for each of the t_1 increments. The spectral width was 50 kHz in both dimensions, and 1024 data complex points were acquired in t_1. One thousand twenty-four t_1 increments were recorded using the TPPI method for sign discrimination in t_1, except for the DREAM experiment where 730 t_1 increments were acquired. The cross-polarization time was 1 ms with a proton field of 100 kHz. The rf field amplitude for all hard pulses was set to 100 kHz (5 μs 180° pulse). The shape of the amplitude in the DREAM experiment is described by $\omega_1(t) = \bar{\omega}_1 - \beta \tan(\alpha[\tau/2 - t])$ with $\alpha = 2 \arctan(\Delta/\beta)/\tau$, $\tau = 8$ ms, $\beta/(2\pi) = 1$ kHz, and $\Delta/(2\pi) = 3$ kHz. The shape of the phase and amplitude of the adiabatic pulses in the TOBSY experiment (WiW9$_{30}^{1}$ pulse sequence using WURST-q pulses) are described by $\omega_1(t) = \omega_1(1 - |\sin(t\pi/T_p)|^q)$ and $\ddot{\phi}(t) = (\omega_1)^2/Q_0$, with $q = 4$, $Q_0 = 5$, $T_p = 55$ μs, and $\omega_1 = 90$ kHz. During

(19) Ernst, M.; Samoson, A.; Meier, B. H. *Chem. Phys. Lett.* **2001**, *348*, 293−302.
(20) Schmidt-Rohr, K.; Spiess, H. W. *Multidimensional Solid-State NMR and Polymers*; Academic Press: London, 1994.
(21) Bennett, A. E.; Rienstra, C. M.; Auger, M.; Lakshmi, K. V.; Griffin, R. G. *J. Chem. Phys.* **1995**, *103*, 6951−6958.
(22) Detken, A.; Hardy, E. H.; Ernst, M.; Meier, B. H. *Chem. Phys. Lett.* **2002**, *356*, 298−304.
(23) Sakellariou, D.; Brown, S. P.; Lesage, A.; Hediger, S.; Bardet, M.; Meriles, C. A.; Pines, A.; Emsley, L. *J. Am. Chem. Soc.* **2003**, *125*, 4376−4380.
(24) Tekely, P.; Palmas, P.; Canet, D. *J. Magn. Reson., Ser. A* **1994**, *107*, 129−133.
(25) Ernst, M.; Meier, B. H. Adiabatic Polarization Transfer Methods in MAS Spectroscopy; In *Encyclopedia of NMR*; John Wiley & Sons: New York, 2002; Vol. 9, pp 23−32.
(26) Verel, R. Baldus, M.; Ernst, M.; Meier, B. H. *Chem. Phys. Lett.* **1998**, *287*, 421−428.
(27) Verel, R.; Ernst, M.; Meier, B. H. *J. Magn. Reson.* **2001**, *150*, 81−99.
(28) Ernst, M.; Samoson, A.; Meier, B. H. *J. Magn. Reson.* **2003**, *163*, 332−339.
(29) Grimmer, A. R.; Kretschmer, A.; Cajipe, V. B. *Magn. Reson. Chem.* **1997**, *35*, 86−90.
(30) Langer, B.; Schnell, I.; Spiess, H. W.; Grimmer, A. R. *J. Magn. Reson.* **1999**, *138*, 182−186.
(31) Favier, A.; Brutscher, B.; Blackledge, M.; Galinier, A.; Deutscher, J.; Penin, F.; Marion, D. *J. Mol. Biol.* **2002**, *317*, 131−144.
(32) Galinier, A.; Haiech, J.; Kilhoffer, M. C.; Jaquinod, M.; Stulke, J.; Deutscher, J.; MartinVerstraete, I. *Proc. Natl. Acad. Sci. U.S.A.* **1997**, *94*, 8439−8444.
(33) Penin, F.; Favier, A.; Montserret, R.; Brutscher, B.; Deutscher, J.; Marion, D.; Galinier, A. *J. Mol. Microbiol. Biotechnol.* **2001**, *3*, 429−432.
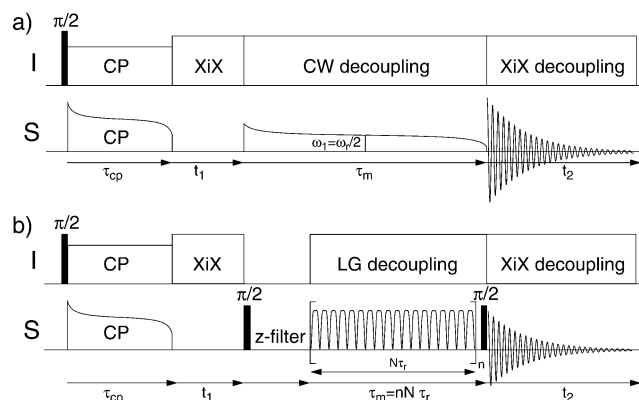(34) Moorsel, G. J. M. P.; Vaneck, E. R. H.; Grey, C. P. *J. Magn. Reson., Ser. A* **1995**, *113*, 159−163.

Figure 1. Pulse sequences for 2D correlation spectra using (a) the DREAM mixing sequence and (b) the TOBSY sequence.
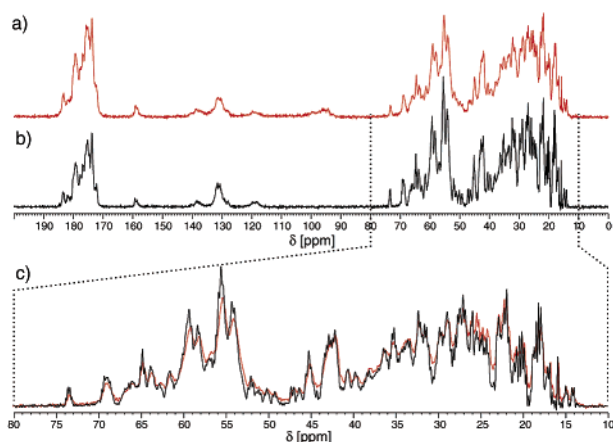

Figure 2. One-dimensional ^{13}C spectra of Crh (a) at 12 kHz MAS frequency and 80 kHz decoupler field strength using TPPM decoupling (τ_p = 5.7 μs, $\Delta\phi$ = 15°) and (b) at 30 kHz MAS frequency and 150 kHz XiX decoupling (τ_p = 95 μs). For each spectrum, 1024 scans were added up with a recycle delay of 3 s, leading to a total acquisition time of about 1 h. (c) Comparison of the aliphatic region of two ^{13}C spectra. The 12 kHz MAS spectrum is shown in red while the 30 kHz MAS spectrum is shown in black.

mixing, the decoupling field was set to 100 kHz for the TOBSY as well as for the DREAM experiment. At 30 kHz MAS frequency, XiX decoupling with a field strength of 150 kHz and a pulse length of 95 μs was used, while at 12 kHz MAS, TPPM decoupling with a field strength of 80 kHz, a pulse length of 5.7 μs, and a phase angle of 15° was used. The z-filter in the TOBSY experiment had a length of 2 ms. The recycle delay was set to 3 s, leading to an acquisition time of about 70 h. The spectra were Fourier-transformed using a cosine-square window function with zero filling to 8 k data points in both dimensions. No baseline correction or resolution enhancement was applied. The pulse sequences for the 2D correlation spectra using the DREAM experiment and the TOBSY experiment are shown in Figure 1a and 1b, respectively.

Results and Discussion

Figure 2 compares the ^{13}C spectrum of Crh at "mild conditions" of 12 kHz MAS and 80 kHz decoupling field (Figure 2a) with the spectrum under "fast MAS" conditions of 30 kHz MAS and 150 kHz decoupling (Figure 2b). The sample temperature was 5 ± 5 °C. The "mild conditions" correspond to typical experimental conditions used for 4-mm o.d. MAS rotors. A comparison of the dispersion of the signals in the aliphatic region of the two spectra shown in Figure 2c shows that indeed no sample deterioration was caused by the high MAS
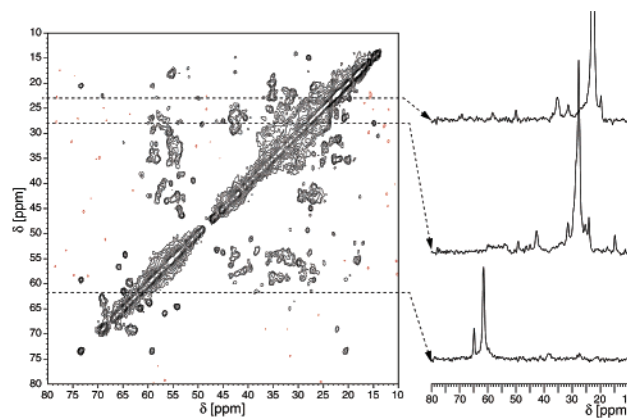

Figure 3. Proton-driven spin-diffusion spectrum recorded at 12 kHz MAS using TPPM decoupling (τ_p = 5.7 μs, $\Delta\phi$ = 15°) with a field strength of about 80 kHz. The mixing time was 10 ms. One thousand twenty-four t_1 increments with 80 scans each were accumulated in approximately 70 h. The contours are spaced logarithmically with a factor of 1.5 between two contours.

frequency and the higher proton decoupling field strength. On the contrary, the spectrum recorded at 30 kHz MAS shows a notably better resolution. We have, however, observed that the resolution depends also on the sample temperature, and therefore, we stop short of claiming higher resolution in the spectrum at 30 kHz from the data presented here. Further experimental evidence will be needed to clearly distinguish between these two effects. Regardless, these measurements clearly illustrate that it is possible to acquire spectra of Crh under "fast MAS" conditions without changes in the structure of the protein.

The most common experiment to obtain homonuclear chemical-shift correlation spectra in peptides and proteins is currently proton-driven spin diffusion (for a review of the method, see ref 35). This experiment has the advantage that no rf irradiation is present during the mixing time of the experiment. It works best at lower MAS frequencies since MAS averages out the homonuclear dipolar couplings among the protons which mediate the ^{13}C−^{13}C polarization transfer,[36] although it can easily be adapted to faster MAS by applying low-power proton irradiation at the HORROR[37] or rotary resonance[38] conditions. A 2D proton-driven spin-diffusion ^{13}C chemical-shift correlation spectrum of Crh with a mixing time of 10 ms is shown in Figure 3. The spectrum was recorded under "mild conditions" with 12 kHz MAS and a decoupler field strength of 80 kHz. The spectrum shows, as expected, clear cross-peaks, but the cross sections shown here illustrate that their intensity is relatively low because polarization transfer is incomplete. The intense diagonal peaks obscure some of the cross-peaks located close to the diagonal.

Alternatively, we have applied the adiabatic DREAM[26,27] polarization transfer sequence as shown in Figure 1a. This sequence belongs to the class of rf-driven polarization transfer sequences[36] and works also in the absence of a coupling to the proton bath. The method requires ^{13}C rf irradiation during the mixing time, however, at low intensity near the HORROR

(35) Ernst, M.; Meier, B. H. Spin Diffusion in Solids. In *Solid State NMR of Polymers*; Ando, I., Asakura, T. Eds.; Elsevier: The Netherlands, 1998.
(36) Meier, B. H. Polarization Transfer and Spin Diffusion in Solid-State NMR. In *Advances in Magnetic and Optical Resonance*; Warren, W. S., Ed.; Academic Press: New York, 1994; Vol. 18, pp 1−116.
(37) Nielsen, N. C.; Bildsoe, H.; Jakobsen, H. J.; Levitt, M. H. *J. Chem. Phys.* **1994**, *101*, 1805.
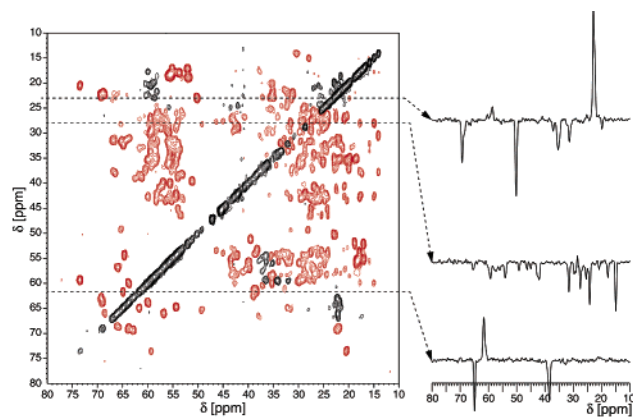(38) Oas, T. G.; Griffin, R. G.; Levitt, M. H. *J. Chem. Phys.* **1988**, *89*, 692.

Figure 4. DREAM spectrum recorded with an adiabatic sweep through the resonance condition at 30 kHz MAS using XiX decoupling ($\tau_p = 95$ μs) with a field strength of about 150 kHz. The mixing time was set to 8 ms. Seven hundred thirty τ_1 increments with 80 scans each were accumulated in approximately 48 h. The contours are spaced logarithmically with a factor of 1.5 between two contours.

Figure 5. TOBSY spectrum recorded with adiabatic pulses at 30 kHz MAS using XiX decoupling ($\tau_p = 95$ μs) with a field strength of about 150 kHz. The mixing time was set to 10 ms. One thousand twenty-four τ_1 increments with 80 scans each were accumulated in approximately 70 h. The contours are spaced logarithmically with a factor of 1.5 between two contours.

condition ($\omega_1 = \omega_r/2$), and heating through the rf irradiation of the recoupling sequence is negligible. The bandwidth of the DREAM recoupling increases with increasing MAS frequency.[27] A 2D DREAM spectrum of Crh at a MAS frequency of 30 kHz is shown in Figure 4. The same number of FIDs (80) were added per t_1 increment as for Figure 3, and the mixing time was set to 8 ms. DREAM is a double-quantum recoupling sequence leading to a negative sign of the cross-peaks for single-step transfers. In comparison to the spin-diffusion spectrum, the intensity of the cross-peaks is greatly enhanced at the cost of the intensity of the diagonal peaks. Cross-peaks much closer to the diagonal of the spectrum can be identified. These observation are best verified in the cross sections through the 2D spectrum, which show significantly higher cross-peak intensities and better S/N than the cross sections through the spin-diffusion spectrum. The S/N ratio of one-bond cross-peaks averages to about 15:1 in the DREAM spectrum at 30 kHz and 4:1 in the spin-diffusion spectrum at 12 kHz MAS. For the DREAM spectrum, the carrier frequency of the ^{13}C channel was placed in the center of the aliphatic region to achieve good recoupling over the full range of aliphatic carbon resonances. At 30 kHz MAS, the bandwidth of the DREAM experiment is not quite sufficient to cover the full range of carbon resonances, and cross-peaks to the carbonyl resonances are weak. These cross-peaks could be observed with an additional DREAM experiment with a different choice of the rf carrier frequency. With increasing MAS frequencies, it will also be possible to obtain DREAM recoupling over the full chemical-shift range of the carbon resonances.

For the assignment of the resonances, the use of through-bond total-correlation experiments (TOBSY),[39,40] as shown in Figure 1b, is a valuable alternative to through-space dipolar-coupling-based experiments. TOBSY transfer is achieved through the isotropic J-coupling by suppressing all anisotropic interactions. A 2D TOBSY spectrum with adiabatic inversion pulses in the mixing sequence[41] is shown in Figure 5. The mixing time was 10 ms, and the rf field strength for the ^{13}C-TOBSY sequence was about 100 kHz. The number of scans

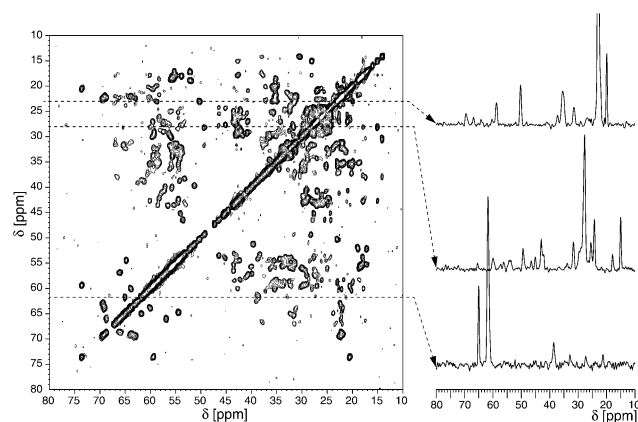is the same as for the spectra in Figures 3 and 4. The bandwidth of the TOBSY sequence is large enough to allow recoupling over the entire range of carbon chemical shifts. Recoupling through the J-coupling is a zero-quantum process, and the cross-peaks have the same sign as the diagonal peaks. There are, however, significantly more cross-peaks in the 2D TOBSY spectrum (Figure 5) than in the 2D spin-diffusion spectrum of Figure 3, and the cross-peaks have higher intensities, averaging to a S/N ratio of 12:1 for the directly bonded carbons.

Conclusions

We have shown that fast MAS at 30 kHz can be safely applied to a microcrystalline protein sample, and that recently developed pulse sequences available only for fast MAS allow us to record 2D homonuclear chemical-shift correlation spectra with significantly improved signal-to-noise ratios. Through-bond as well as through-space transfer can be realized under these conditions. Both experiments lead to significant improvement of the cross-peak S/N ratio compared to spin-diffusion spectra at lower MAS frequencies.

We found that the improved pulse sequences can overcompensate for the lower S/N ratio of spectra from small amounts of sample. Therefore, it is attractive to use smaller rotors even if the amount of compound available is sufficient for a larger rotor. A S/N ratio for the DREAM cross-peaks of 15:1 (for next neighbor cross-peaks) was obtained in about 70 h of experimental time on a sample of 4 mg of protein in a 2.5-mm rotor. We found that the S/N ratio of the cross-peaks in a DREAM experiment using a 2.5-mm rotor is almost two times higher than the cross-peaks in a spin-diffusion experiment using a full 4-mm rotor. This improvement is primarily based on the higher polarization transfer efficiency of the DREAM sequence most easily realized under fast MAS conditions. We expect that similar considerations apply for even smaller rotor diameters and correspondingly higher MAS frequencies.

(39) Baldus, M.; Meier, B. H. *J. Magn. Reson., Ser. A* **1996**, *121*, 65−69.
(40) Hardy, E. H.; Verel, R.; Meier, B. H. *J. Magn. Reson.* **2001**, *148*, 459−464.
(41) Detken, A.; Hardy, E.; Meier, B. H. *J. Magn. Reson.* **2003**, *165*, 208−218.